

Non-Abelian $\nu = 1/2$ quantum Hall state in Γ_8 Valence Band Hole Liquid

George Simion* and Yuli Lyanda-Geller†

Department of Physics and Astronomy and Purdue Quantum Center,
Purdue University, West Lafayette IN, 47907 USA

(Dated: March 10, 2016)

In search of states with non-Abelian statistics, we explore the fractional quantum Hall effect in a system of two-dimensional charge carrier holes. We propose a new method of mapping states of holes confined to a finite width quantum well in a perpendicular magnetic field to states in a spherical shell geometry. This method provides single-particle hole states used in exact diagonalization of systems with a small number of holes in the presence of Coulomb interactions. An incompressible fractional quantum Hall state emerges in a hole liquid at the half-filling of the ground state in a magnetic field in the range of fields where single-hole states cross. This state has a negligible overlap with the Halperin 331 state, but a significant overlap with the Moore-Read Pfaffian state. Excited fractional quantum Hall states for small systems have sizable overlap with non-Abelian excitations of the Moore-Read Pfaffian state.

Quasiparticles obeying non-Abelian statistics lead to fault tolerant quantum computing [1–3]. Exotic states resulting in non-Abelian excitations can arise in low dimensional quantum liquids in the presence of magnetic fields. The fractional quantum Hall (FQH) state in a two-dimensional (2D) electron liquid at filling factor $\nu = 5/2$ is the state most studied theoretically and possibly observed experimentally [4–7]. There are other FQH states at $\nu = 12/5$ [8] and $\nu = 8/3$ [8–10], bilayer $\nu = 1/2$ 2D electron phase [11–14], and $\nu = 1/4$ state [15, 16], for which non-Abelian origin of excitations has been discussed. Other candidates for non-Abelian systems are vortices in p -wave superconductors [17], and hybrid systems with proximity-induced s -wave superconductivity that mimic a p -wave pairing in semiconductors and topological insulators, due to spin-orbit coupling [18, 19], Dirac spectra [20], or Laughlin anyon quasiparticles [21].

Here we show that FQHE in 2D hole systems is a new promising non-Abelian setting. Luttinger valence band holes are fundamentally different from electrons. They exhibit non-Abelian phases in transport even for single-hole states [22]. In a magnetic field, the single-hole states are four-component spinors. Each spinor component is described by a distinct Landau level (LL) wavefunction u_n , $n \geq 0$. The relative weights of these functions in spinors vary with magnetic field [23]. Functions u_1 generating FQH non-Laughlin electron correlations [24] have sizable weight in several hole states. Furthermore, the hole ground state in certain ranges of magnetic field is not defined by u_0 , like for electrons, but by $u_{n \neq 0}$, including u_1 . Thus, the non-Abelian FQH hole states can arise when the ground level in a single quantum well is filled.

Compared to electrons, holes have smaller cyclotron energy and stronger LL mixing by Coulomb interactions. Single-hole magnetic spectra exhibit multiple level crossings, particularly in the ground state. Near crossings, ratio of interaction and cyclotron energies changes significantly for relatively small changes in magnetic field, and interaction pseudopotentials can be easily controlled.

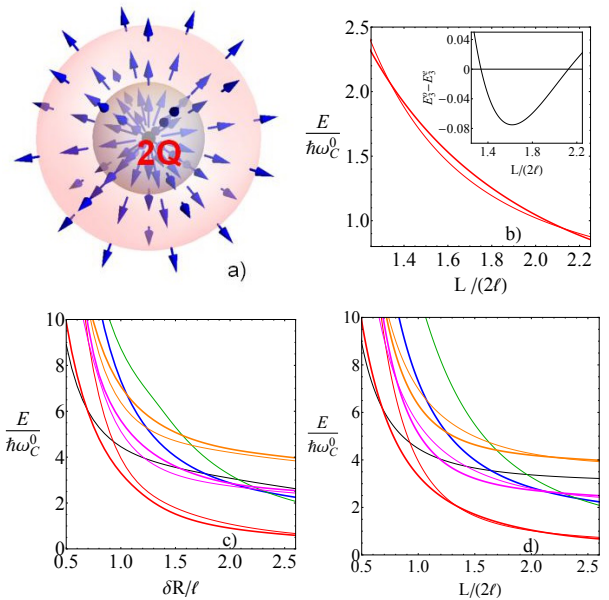


FIG. 1: Color online: a - Spherical shell geometry; b - Ground state level crossings in a spherical shell (red solid lines) and planar geometry (black dotted lines); c,d - lowest nine states spectra ($n \leq 5$) in a spherical shell geometry with $Q = 100$ (c) and planar geometry (d). The highest index Landau wavefunction in four-spinors of the shown hole states: Black lines - u_0 ; blue - u_1 ; green - u_2 ; red - u_3 ; magenta - u_4 ; orange - u_5 . Thick lines- even states, thin lines-odd states. The thin red line state spinor has significant u_1 -component.

A strong overlap, like for electrons at $\nu = 5/2$ [25], is then possible with Moore-Read [4] or anti-Pfaffian states [26]. Control of LL mixing was discussed for crossing of electron levels dominated by u_0 and u_1 , when $\nu = 2/5$ electron liquid is tuned by a small change in magnetic field from a Laughlin state to a state with non-Laughlin correlations and non-Abelian excitations [2]. However, such electron cases are rare. Spectral crossings for holes are numerous, which makes the phase diagram for hole liquid much richer than that for electrons.

In search of non-Abelian hole states we propose a theo-

retical framework for treatment of FQHE in hole systems. Unusual hole spectra in magnetic field arise from strong coupling between the in-plane and spatial quantization z -direction motion in a quantum well, caused by strong spin-orbit interactions. Hole four-spinors and the inseparability of the in-plane and z -direction degrees of freedom make the treatment of Coulomb interactions challenging. For electrons, the in-plane and z -direction motion are independent, so it is possible to use the Haldane technique[27] of homogeneous states with translationally invariant wavefunctions for a finite number of electrons on a sphere in a monopole magnetic field. This method cannot be applied to holes. We propose a new method of mapping quantum well confined hole states in a spherical shell geometry, Fig. 1. We then use our method for consideration of the $\nu = 1/2$ hole state at quantum well widths corresponding to the range of magnetic fields with ground hole state crossings. We demonstrate that the FQH state at $\nu = 1/2$ is not the Halperin 331 state [28] but rather a Moore-Read (MR) state.

Holes in a planar and spherical shell geometry. The Luttinger Hamiltonian [29] in magnetic field \mathbf{B} is

$$\hat{H}_0 = \left(\gamma_1 + \frac{5}{2}\gamma \right) \frac{\hat{\mathbf{k}}^2}{2} I - \gamma \left(\hat{\mathbf{k}} \cdot \mathbf{s} \right)^2 - \left(\frac{\gamma}{2} + \kappa \right) s_z, \quad (1)$$

where energies are in units of a free electron cyclotron energy $\hbar\omega_c^0 = \hbar eB/m_0c$, dimensionless coordinates \mathbf{r} are in units of magnetic length ($\ell = \sqrt{\hbar c/eB}$), wavevectors $\mathbf{k} = -i\nabla_{\mathbf{r}} + e\ell\mathbf{A}/(\hbar c)$, \mathbf{A} is the vector potential, \mathbf{s} is spin 3/2 operator, and γ_1 , γ and κ are Luttinger parameters in a spherical approximation. This Hamiltonian commutes with the z -projection of total angular momentum $j_z = l_z + s_z$, l is the angular momentum. In a symmetric gauge, the hole wavefunctions in a quantum well of width L are:

$$\Psi_{n,m}^{\{\alpha\}} = \begin{pmatrix} \zeta_0^{\{\alpha\}}(z)u_{n,m} \\ \zeta_1^{\{\alpha\}}(z)u_{n-1,m+1} \\ \zeta_2^{\{\alpha\}}(z)u_{n-2,m+2} \\ \zeta_3^{\{\alpha\}}(z)u_{n-3,m+3} \end{pmatrix}, \quad (2)$$

where $u_{n,m}$ are symmetric gauge eigenfunctions[30], and $\zeta(z)$ are envelope functions satisfying the boundary conditions $\Psi(\pm L/2) = 0$. These wavefunctions reflect the correlation of the in-plane and z -direction motion, leading to a mutual transformation of heavy and light holes at the heterointerfaces due to giant spin-orbit coupling. Energies and wavefunctions are characterized by a single length scale $w = L/(2\lambda)$ [23]. For $n < 3$, the components of wavefunctions with $n - l < 0$, $l = 1, 2, 3$ vanish, and $n + 1$ components are nonzero. The wavefunctions are even or odd in respect to reflection about a plane $z = 0$.

In order to construct homogeneous states with translationally invariant wavefunctions, we confine holes to a spherical shell with radius $R_0 - \delta_R \leq r \leq R_0 + \delta_R$ as shown schematically in Fig. 1 a. A magnetic field

$B = 2Qhc/(4\pi er^2)$, is related to an integer monopole of strength $2Q$, so that magnetic flux through spherical surfaces around it $\phi = 2Qhc/e$. Because $\mathbf{j} = \mathbf{l} + \mathbf{s}$ is a good quantum number for single-hole states, the eigenfunctions of (1) for a spherical shell are

$$\psi_{\alpha jm}(r, \theta, \phi) = \sum_{l=j-\frac{3}{2}}^{l=j+\frac{3}{2}} R_{\alpha j}^l(r) \times \begin{pmatrix} \langle j, m | l, m - \frac{3}{2}; \frac{3}{2}, +\frac{3}{2} \rangle Y_{Q,l,m-\frac{3}{2}}(\theta, \phi) \\ \langle j, m | l, m - \frac{1}{2}; \frac{3}{2}, +\frac{1}{2} \rangle Y_{Q,l,m-\frac{1}{2}}(\theta, \phi) \\ \langle j, m | l, m + \frac{1}{2}; \frac{3}{2}, -\frac{1}{2} \rangle Y_{Q,l,m+\frac{1}{2}}(\theta, \phi) \\ \langle j, m | l, m + \frac{3}{2}; \frac{3}{2}, -\frac{3}{2} \rangle Y_{Q,l,m+\frac{3}{2}}(\theta, \phi) \end{pmatrix}, \quad (3)$$

where $\langle j, m_j | l, m - l; \frac{3}{2}, m_s \rangle$ are the Clebsch-Gordan coefficients of $\mathbf{j} = \mathbf{l} + \mathbf{s}$, $Y_{Q,l,m}$ are the monopole harmonics [31], and α labels subbands. Radial functions $R_{\alpha j}^l(r)$ are defined by the boundary conditions $\psi_{\alpha jm}(R_0 \pm \delta_R) = 0$. Each wavefunction (3) contains up to four spinors, each spinor having four components. The monopole harmonics are defined if $l \geq Q$ [31], so that $2j \geq 2Q - 3$. For the states with $2j < 2Q + 3$, $j - Q + 5/2$ spinor components are nonzero, while for $2j \geq 2Q + 3$ all components of spinors are non-zero. In Figs. 1 c and d we present hole spectra in spherical and planar geometries. Each band of states includes two states for every $2j \geq (2Q + 3)$.

The energy spectra in the planar and spherical shell geometry are almost identical, and crossings of the corresponding states in both geometries occur almost at the same ratio w . Energies in a spherical shell converge to the planar limit for very large Q in much the same way as the Haldane electron wavefunctions on the sphere converge to their planar limit. We note that for finite Q , there is no even-odd reflection parity, but it is restored in the large Q limit. Fig. 2 c-d, shows radial distributions of charge for the lowest states of the quantum well. The radial distribution of charge density converges to the planar limit at large Q . Thus, mapping of quantum well holes over a spherical shell provides one to one correspondence between states. Each spherical state with total angular momentum j corresponds to a planar state characterized by index $n = j - Q + 3/2$. Each spinor of spherical wavefunctions with angular momentum l corresponds to a spin component in the planar geometry with $s_z = j - l$, and the radial wavefunctions are spherical equivalents of the z -envelope functions of the planar geometry.

Crucially, hole states mix different functions $u_n(r)$. Fig. 2d shows that u_0 favoring Laughlin electron correlations dominates $n = 3$ even hole planar state and its spherical counterparts. However, u_1 , favoring non-Laughlin correlations and non-Abelian excitations, is prominent in other hole states. The weights of these functions for hole spinors depend on w , and can be changed significantly by a slight change of a magnetic field.

Coulomb Interactions. A system of identical charged particles in a magnetic field is highly degenerate. The Coulomb interaction cannot be treated perturbatively.

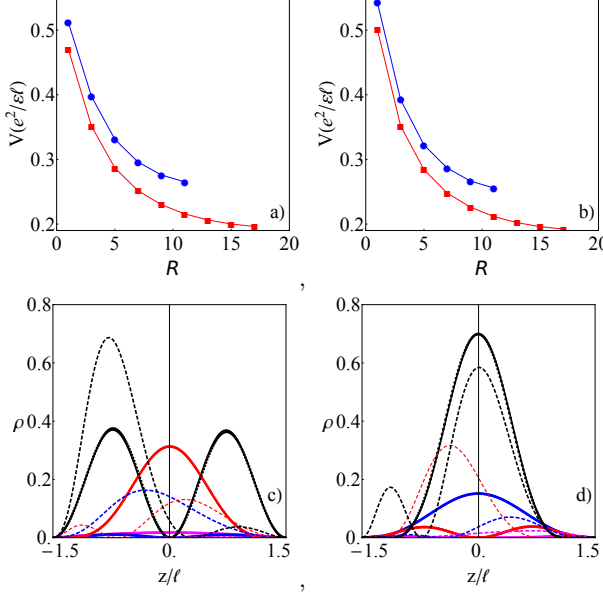


FIG. 2: Color online. a,b: pseudopotentials for $w = 1.6$ for $2Q = 10$ (blue dots) and $2Q = 15$ (red squares) for odd $n = 3$ state (a), and even $n = 3$ state (b). c,d: The charge density ρ . Vertical axis is for odd $n = 3$ state (c) and for even $n = 3$ state (d). Black line: $-3/2$ spin component (containing $u_0(r)$), red line: spin $-1/2$ spin component (containing $u_1(r)$), magenta: $1/2$ spin component (containing $u_2(r)$) blue: spin $3/2$ (containing $u_3(r)$). The odd state has a bigger u_1 admixture and its pseudopotential resembles that of LL1 electrons, while the even state pseudopotential resembles that of LL0 electrons. In c and d, dashed lines correspond to $Q = 15$, dotted lines represent $Q = 10^8$ and solid lines are for the planar case.

Such systems are modeled using a small number of particles. We perform exact diagonalization of Coulomb interactions $H_i = \sum_{ij} \frac{e^2}{\epsilon r_{ij}}$ for holes in a spherical shell geometry and discuss extrapolation to the thermodynamic limit. The single-particle Hilbert space is defined by states (3). The many-body basis set is given by all wavefunctions obtained when N holes are placed in single-particle states. We calculate the Coulomb interactions matrix elements using addition of angular momenta. Their explicit expressions and a system of differential equations for radial components of wavefunctions are presented in the Supplementary Material.

The integral of motion in our many-body system is the total angular momentum $\mathbf{J} = \sum_i \mathbf{j}_i$ and its z -projection. We apply the Wigner-Eckart theorem [32]

$$\langle J', M', \beta' | H_i | J, M, \beta \rangle = \delta_{JJ'} \delta_{MM'} V_{\beta\beta'}(\mathcal{J}), \quad (4)$$

and reduce the Hilbert space, by using independence of interaction matrix elements on the z -projection of the total angular momentum of all holes, J_z . Here index β labels the multiplets of many-body states with the same total J and the same total M , and $V_{\beta\beta'}(J) = \langle J', \beta' | H_i | J, \beta \rangle$ are the pseudopotentials [27]. We first compute the principal contribution to the two-body pseu-

dopotentials of two holes, each with an angular momentum j , without including any virtual transitions to other states, $V_{00}^0(\mathcal{J} = \mathbf{j} + \mathbf{j}) \equiv V_0(\mathcal{R})$, where $\mathcal{R} = j_1 + j_2 - J$ is the relative angular momentum. For the two-body interactions, there is one multiplet for each allowed value of \mathcal{J} . The two-hole pseudopotentials $V_0(\mathcal{R})$ are shown in Fig. 2a-b for holes whose wavefunctions are the spherical counterparts of the odd parity $n = 3$ planar state, and the even parity $n = 3$ planar state, correspondingly.

Landau level mixing. The hole liquid LL mixing strength parameter $e^2/(\ell \hbar \omega_C)$ is very large, so we include hole virtual transitions to the other states. First, we construct a basis set with \mathcal{J} in the two-hole state, with both holes in the same single-hole state. Holes undergo virtual transitions to excited levels in a certain range of energy. A similar method was used for electrons [33, 34]. We diagonalize the Coulomb interaction in this basis. The lowest energy acts as an effective interaction. In this work, we include virtual transitions into 17 excited states that span the range of energy $4\hbar\omega_C$ [35] due to non-regular separation between hole states. The results are corrections δV to the two-hole pseudopotentials $V_0(\mathcal{R})$. Differences between δV at different \mathcal{R} in units of $e^4/(\ell \epsilon)^2/(\hbar \omega_C^0)$ are shown in Fig. 3a.

We next find the three-body pseudopotentials $V_{00}(\mathcal{J})$, $\mathcal{J} = \mathbf{j} + \mathbf{j} + \mathbf{j}$ due to LL mixing. For pseudopotentials at $\mathcal{R}_3 = 3j - J < 9$ each value of \mathcal{J} is characterized by only one multiplet. The basis set is made of the three-hole states, comprised of single-hole states with energy up to $4\hbar\omega_C$. Using the same procedure as in the two-hole case, we find an effective three-body pseudopotential. We then have extracted its irreducible part $\tilde{V}(\mathcal{R}_3)$, by subtracting the ground state energy of a three-hole system, whose interactions are given by the two-body pseudopotentials determined above. A similar procedure was used for electrons [36]. Differences between \tilde{V} at different \mathcal{R}_3 in units of $e^4/(\ell \epsilon)^2/(\hbar \omega_C^0)$ are shown in Fig. 3b. Tables of the two- and three-body pseudopotentials in the $Q \rightarrow \infty$ limit are given in the Supplementary Material.

$\nu = 1/2$ state. We now consider FQHE for $\nu = 1/2$ of the ground hole state. For electrons, an incompressible state at filling factor ν in LL0 is obtained for a system with N particles placed on an angular momentum shell of $2l = \nu^{-1}N + \delta$, where δ is the finite size shift given by a topological quantum number describing the nature of correlations [37, 38], and $l = Q + n$. For electrons at $\nu = 1/2$, $\delta = -3$, and this value is used to describe $\nu = 5/2$ state in the LL1 [39]. For Luttinger holes, several Landau indices define the spinors characterizing the two lowest states, and the results for electron δ [37, 38] are not applicable directly. However, our simulation shows that for holes, $\delta = -3$ leads to an incompressible state at $n = 6, 8, 10, 12$, so that the total j satisfies $2j = 2N - 3$ and the magnetic monopole is $2Q = 2j - 3$. The incompressible ground state persists in the entire range $1.3 < w < 2.2$, that includes ground

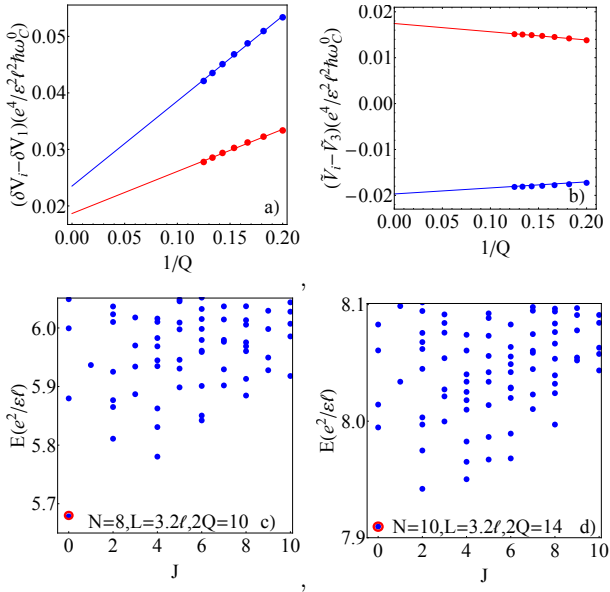


FIG. 3: Color online: a. LL mixing corrections to the two-hole pseudopotentials. Red: $\delta V(\mathcal{R} = 3) - \delta V(\mathcal{R} = 1)$; blue: $\delta V(\mathcal{R} = 5) - \delta V(\mathcal{R} = 1)$, $w = 1.6$. b. Three-hole irreducible pseudopotentials. Red: $\tilde{V}(\mathcal{R}_3 = 5) - \tilde{V}(\mathcal{R}_3 = 3)$; blue: $\tilde{V}(\mathcal{R}_3 = 6) - \tilde{V}(\mathcal{R}_3 = 3)$, $w = 1.6$. c,d. Spectra for 8 and 10 holes at $\nu = 1/2$. $J = 0$ ground state separated by a gap indicates an incompressible state.

state crossings of the two lowest $n = 3$ levels shown in Fig. 1b. (We also tested that $\delta = -1$ does not result in an incompressible states).

We first investigate whether the experimentally observed FQH state [40] is of the 331 type. The Halperin 331 state arises when there are two species of interacting electrons, such as, e.g., electrons in a bilayer system. The two candidates for the degenerate species in hole FQHE are $n = 3$ odd and $n = 3$ even states near and at their crossings. A translationally invariant wavefunction of the 331 state was found in [41] using the confinement of two species of fermions to the surface of the sphere with a monopole magnetic field in the center. Pseudopotential describing interactions between fermions of the same species has a repulsive character for $\mathcal{R} = 1$ and zero for all other \mathcal{R} . Interaction between fermions of different species is repulsive for $\mathcal{R} = 0$. The same construction has been generalized for systems containing two different types of fermions, e.g., bilayer electron liquid [13]).

Using the spherical shell configuration, we calculate the wavefunction at $\nu = 1/2$. For modeling the 331 state, the many-hole Hilbert space must be made of the lowest states of the double degenerate system. Its size is very large even for small systems ($\approx 10^6$ for 10 particles). Spinor single-hole states further complicate the simulation. Unlike the electron spin, the hole spin is not a good quantum number. The pseudospin comprised of the spherical shell counterparts of the planar $n = 3$ odd and $n = 3$ even states is not conserved in the presence of

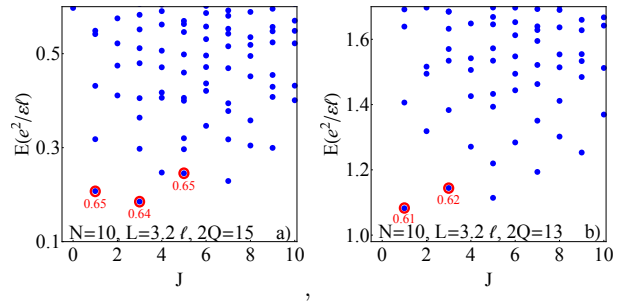


FIG. 4: Quasiholes (left) and quasielectron (right) pair excitations of $\nu = 1/2$ for $N = 10$. Values of overlap between low lying excitations (red circles) and the corresponding Moore-Read excitations are shown.

the Coulomb interactions. Furthermore, quantum number J does not uniquely specify a state for three holes. This makes the simulation very challenging, and we limit it to 8 holes interacting within the Hilbert space defined by the two crossing single-hole levels. The exact diagonalization of the Coulomb interactions indicates that an incompressible $J = 0$ ground state is present for w in the whole range of magnetic fields that includes two crossings shown in inset of Fig. 1b. However, the overlap of the corresponding hole wavefunction with the 331 wavefunction [41] is only 0.165 – 0.17 in the whole range of fields. It was suggested for the bilayer system [42] that absence of tunneling favors the 331 state. In the present case, there is no single-particle tunnel splitting at the crossings. However, even at crossings, there is significant hole-hole interactions induced mixing of crossing levels, analog of tunneling, because of the non-conservation of the "pseudospin" comprised of $n = 3$ odd and $n = 3$ even hole states. That precludes the possibility that the wavefunction of a many-hole system in thermodynamic limit will correspond to the Halperin 331 state.

We now consider a Moore-Read state favored by significant weight of u_1 in the ground state hole spinor. In our case a simulation of $N = 6$ and $N = 12$ hole systems cannot be reliably used: besides $\nu = 1/2$, they can equally well describe filling factors $\nu = 2/3$ and $\nu = 3/5$, respectively. Systems with $N \geq 14$ holes are too large for available computational resources, and we restrict to $N = 8, 10$ holes confined to a spherical shell. The many-body basis is built using the hole ground state, including the LL mixing. By nature of the spherical shell approach for holes, the effect of a finite width of the quantum well is taken into account. The exact diagonalization (Fig. 3 c-d) shows a $J = 0$ ground state separated by a gap from the continuum of states, a clear indication of an incompressible state at $\nu = 1/2$. The maximal gap occurs at $w = 1.6$, very close to w in experiments [40]. The overlap with the MR ground state[43] at $B = 10T$ is 0.8 for $N = 8$ and 0.62 for $N = 10$. Excitations of FQH systems arise when flux quanta are added or subtracted. Here adding one flux quantum in the ground state cre-

ates two quasiholes excitations, and subtracting one flux quantum gives two quasielectrons. MR quasiholes obey non-Abelian statistics [4]. We compare excited states for $N = 10$ hole system with the MR excitations, Fig. 4. The overlap with excitations of the MR state ~ 0.65 , indicating that this FQH hole system possibly has non-Abelian statistics of excitations. Higher magnetic fields (at the same w) reduce LL mixing and enhance the MR state. At $B = 16T$, $L = 200$ Å, the overlap with MR state for $N = 10$ is 0.7.

Conclusion. We proposed the method of investigation of the finite size quantum Hall systems of valence band holes in a spherical shell geometry. Our simulations show the incompressible FQH state at $\nu = 1/2$ of the ground state of holes in magnetic field. The hole liquid at $\nu = 1/2$ is not in the Halperin 331 state but is rather described by the Moore-Read type of correlations in the many-body ground state, with excitations having sizable overlap with the Moore-Read Pfaffian excitations. Experimentally, besides direct interference tests aimed at discovery of non-Abelian statistics [1, 6], it is of interest to compare transport characteristics of $\nu = 1/2$ hole state and $\nu = 5/2$ electron state in high magnetic fields. Future work includes modeling systems with a larger number of holes, study of FQHE at other filling factors, probing exotic states, such as the interlayer Pfaffian [44], and evaluation of entanglement entropy for hole FQH systems [45, 46]. This work is supported by the U.S. Department of Energy, Office of Basic Energy Sciences, Division of Materials Sciences and Engineering under Award de-sc0010544.

* Electronic address: simion@purdue.edu

† Electronic address: yuli@purdue.edu

- [1] C. Nayak, S. H. Simon, A. Stern, M. Freedman, and S. Das Sarma, *Rev. Mod. Phys.* **80**, 1083 (2008).
- [2] L. Hormozi, N. E. Bonesteel, and S. H. Simon, *Phys. Rev. Lett.* **103**, 160501 (2009).
- [3] S. Das Sarma, M. Freedman, and C. Nayak, *Phys. Rev. Lett.* **94**, 166802 (2005).
- [4] G. Moore and N. Read, *Nuclear Physics B* **360**, 362 (1991).
- [5] N. Read and D. Green, *Phys. Rev. B* **61**, 10267 (2000).
- [6] R. L. Willett, *Reports on Progress in Physics* **76**, 076501 (2013).
- [7] R. Willett, J. P. Eisenstein, H. L. Störmer, D. C. Tsui, A. C. Gossard, and J. H. English, *Phys. Rev. Lett.* **59**, 1776 (1987).
- [8] N. Read and E. Rezayi, *Phys. Rev. B* **59**, 8084 (1999).
- [9] E. Ardonne, F. J. M. v. Lankvelt, A. W. W. Ludwig, and K. Schoutens, *Phys. Rev. B* **65**, 041305 (2002).
- [10] M. Barkeshli and X.-G. Wen, *Phys. Rev. Lett.* **105**, 216804 (2010).
- [11] Y. W. Suen, L. W. Engel, M. B. Santos, M. Shayegan, and D. C. Tsui, *Phys. Rev. Lett.* **68**, 1379 (1992).
- [12] S. Hasdemir, Y. Liu, H. Deng, M. Shayegan, L. N. Pfeiffer, K. W. West, K. W. Baldwin, and R. Winkler, *Phys. Rev. B* **91**, 045113 (2015).
- [13] M. R. Peterson and S. Das Sarma, *Phys. Rev. B* **81**, 165304 (2010).
- [14] Z. Papić, M. O. Goerbig, N. Regnault, and M. V. Milovanović, *Phys. Rev. B* **82**, 075302 (2010).
- [15] D. R. Luhman, W. Pan, D. C. Tsui, L. N. Pfeiffer, K. W. Baldwin, and K. W. West, *Phys. Rev. Lett.* **101**, 266804 (2008).
- [16] Z. Papić, G. Möller, M. V. Milovanović, N. Regnault, and M. O. Goerbig, *Phys. Rev. B* **79**, 245325 (2009).
- [17] G. E. Volovik, *Fermions in the vortex core in chiral superconductors* (1997), 9709159v3.
- [18] R. M. Lutchyn, J. D. Sau, and S. Das Sarma, *Phys. Rev. Lett.* **105**, 077001 (2010).
- [19] Y. Oreg, G. Refael, and F. von Oppen, *Phys. Rev. Lett.* **105**, 177002 (2010).
- [20] L. Fu and C. L. Kane, *Phys. Rev. Lett.* **100**, 096407 (2008).
- [21] D. J. Clarke, J. Alicea, and K. Shtengel, *Nat. Commun.* **4** (2013).
- [22] D. P. Arovas and Y. Lyanda-Geller, *Phys. Rev. B* **57**, 12302 (1998).
- [23] G. E. Simion and Y. B. Lyanda-Geller, *Phys. Rev. B* **90**, 195410 (2014).
- [24] G. E. Simion and J. J. Quinn, *Physica E: Low-dimensional Systems and Nanostructures* **41**, 1 (2008).
- [25] A. Wójs, C. Tóke, and J. K. Jain, *Phys. Rev. Lett.* **105**, 096802 (2010).
- [26] M. Levin, B. I. Halperin, and B. Rosenow, *Phys. Rev. Lett.* **99**, 236806 (2007).
- [27] F. D. M. Haldane, *Phys. Rev. Lett.* **51**, 605 (1983).
- [28] B. I. Halperin, *Helvetica Physica Acta* **56** (1983).
- [29] J. M. Luttinger, *Phys. Rev.* **102**, 1030 (1956).
- [30] L. Landau and E. Lifshitz, *Quantum Mechanics* (Butterworth-Heinemann, 1981).
- [31] T. T. Wu and C. N. Yang, *Nucl. Phys. B* **107**, 365 (1976).
- [32] A. Edmonds, *Angular Momentum in Quantum Mechanics* (Princeton University Press, 1996).
- [33] S. H. Simon and E. H. Rezayi, *Phys. Rev. B* **87**, 155426 (2013).
- [34] R. E. Wooten, J. H. Macek, and J. J. Quinn, *Phys. Rev. B* **88**, 155421 (2013).
- [35] The cyclotron frequency ω_C corresponds to the semiclassical cyclotron frequency at large n [23].
- [36] E. H. Rezayi and F. D. M. Haldane, *Phys. Rev. B* **42**, 4532 (1990).
- [37] X. Wen and A. Zee, *Phys. Rev. Lett.* **69**, 953 (1992).
- [38] N. d'Ambrumenil and R. Morf, *Phys. Rev. B* **40**, 6108 (1989).
- [39] M. Storni, R. H. Morf, and S. Das Sarma, *Phys. Rev. Lett.* **104**, 076803 (2010).
- [40] Y. Liu, A. L. Graninger, S. Hasdemir, M. Shayegan, L. N. Pfeiffer, K. W. West, K. Baldwin, and R. Winkler, *Phys. Rev. Lett.* **112**, 046804 (2014).
- [41] F. D. M. Haldane and E. H. Rezayi, *Phys. Rev. Lett.* **60**, 956 (1988).
- [42] T. Ho, *Phys. Rev. Lett.* **75**, 1187 (1995).
- [43] M. Greiter, X.-G. Wen, and F. Wilczek, *Phys. Rev. Lett.* **66**, 3205 (1991).
- [44] M. Barkeshli and X.-G. Wen, *Phys. Rev. B* **82**, 233301 (2010).
- [45] J. Shao, E.-A. Kim, F. D. M. Haldane, and E. H. Rezayi, *Phys. Rev. Lett.* **114**, 206402 (2015).
- [46] O. S. Zozulya, M. Haque, K. Schoutens, and E. H. Rezayi, *Phys. Rev. B* **76**, 125310 (2007).

**Supplementary Materials:
Non-Abelian $\nu = 1/2$ quantum Hall state in Γ_8 Valence Band Hole Liquid**

Differential equations for radial components of the hole wavefunctions in a spherical shell in the presence of a magnetic monopole

The radial envelope functions $R(r)$ are solutions of a system of coupled differential equations

$$-\gamma_1 \left[\frac{1}{2} \frac{d^2}{dr^2} + \frac{d}{dr} - \frac{l(l+1) - Q^2}{2r^2} \right] R_{nj}^l(r) + \gamma \left[\mathcal{M}_{ll'}^2 \frac{d^2}{dr^2} + \mathcal{M}_{ll'}^1 \frac{1}{r} \frac{d}{dr} + \frac{\mathcal{M}_{ll'}^0}{r^2} \right] R_{nj}^{l'}(r) = E_{nj} R_{nj}^l, \quad (\text{S1})$$

with boundary conditions $(R_{nj}^l(\pm\delta R) = 0)$. Here matrices \mathcal{M}^i are given by

$$\mathcal{M}^0 = \begin{pmatrix} \frac{\Delta_{-\frac{3}{2}}}{2} \frac{2j-3}{2j} \left(1 - \frac{3\eta_{-\frac{1}{2}}\eta_{-\frac{3}{2}}}{2\Delta_{-\frac{3}{2}}} \right) & (j - \frac{3}{2}) \tilde{u}_1 & \tilde{v}_1 (j + \frac{3}{2}) (j - \frac{1}{2}) & 0 \\ - (j + \frac{1}{2}) \tilde{u}_1 & - \frac{\Delta_{-\frac{1}{2}}}{2} \frac{2j+5}{2j+2} \left(1 - \frac{3\eta_{\frac{1}{2}}\eta_{-\frac{1}{2}}}{2\Delta_{-\frac{1}{2}}} \right) & -\tilde{w} (j - \frac{1}{2}) & \tilde{v}_2 (j + \frac{1}{2}) (j + \frac{5}{2}) \\ \tilde{v}_1 (j - \frac{3}{2}) (j + \frac{1}{2}) & \tilde{w} (j + \frac{3}{2}) & - \frac{\Delta_{\frac{1}{2}}}{2} \frac{2j-3}{2j} \left(1 - \frac{3\eta_{\frac{3}{2}}\eta_{\frac{1}{2}}}{2\Delta_{\frac{1}{2}}} \right) & -\tilde{u}_2 (j + \frac{1}{2}) \\ 0 & \tilde{v}_2 (j - \frac{1}{2}) (j + \frac{3}{2}) & \tilde{u}_2 (j + \frac{5}{2}) & \frac{\Delta_{\frac{3}{2}}}{2} \frac{2j+5}{2j+2} \left(1 - \frac{3\eta_{\frac{5}{2}}\eta_{\frac{3}{2}}}{2\Delta_{\frac{3}{2}}} \right) \end{pmatrix}, \quad (\text{S2})$$

$$\mathcal{M}^1 = \begin{pmatrix} - \frac{2j-3}{2j} \left(1 - 3\eta_{-\frac{3}{2}}\eta_{-\frac{1}{2}} \right) & (2j+3) \tilde{u}_1 & 2\tilde{v}_1 (j+1) & 0 \\ - (2j-5) \tilde{u}_1 & \frac{2j+5}{2j+2} \left(1 - 3\eta_{-\frac{1}{2}}\eta_{\frac{1}{2}} \right) & -\tilde{w} (2j+5) & 2\tilde{v}_2 (j+2) \\ -2\tilde{v}_1 (j-1) & \tilde{w} (2j-3) & \frac{2j-3}{2j} \left(1 - 3\eta_{\frac{3}{2}}\eta_{\frac{1}{2}} \right) & -\tilde{u}_2 (2j+7) \\ 0 & -2\tilde{v}_2 j & \tilde{u}_2 (2j-1) & - \frac{2j+5}{2j+2} \left(1 - 3\eta_{\frac{3}{2}}\eta_{\frac{5}{2}} \right) \end{pmatrix}, \quad (\text{S3})$$

$$\mathcal{M}^2 = \begin{pmatrix} - \frac{2j-3}{4j} \left(1 - 3\eta_{-\frac{3}{2}}\eta_{-\frac{1}{2}} \right) & 2\tilde{u}_1 & \tilde{v}_1 & 0 \\ 2\tilde{u}_1 & \frac{2j+5}{4j+4} \left(1 - 3\eta_{-\frac{1}{2}}\eta_{\frac{1}{2}} \right) & -2\tilde{w} & \tilde{v}_2 \\ \tilde{v}_1 & -2\tilde{w} & \frac{2j-3}{4j} \left(1 - 3\eta_{\frac{3}{2}}\eta_{\frac{1}{2}} \right) & -2\tilde{u}_2 \\ 0 & \tilde{v}_2 & -2\tilde{u}_2 & - \frac{2j+5}{4j+4} \left(1 - 3\eta_{\frac{3}{2}}\eta_{\frac{5}{2}} \right) \end{pmatrix}, \quad (\text{S4})$$

where $\eta_k = s/(j+k)$, $\Delta_k = (j+k)(j+k+1) - Q^2$ and

$$\tilde{u}_1 = \eta_{\frac{1}{2}} \sqrt{\frac{3(1+j)}{4j}} \sqrt{1 - \eta_{-\frac{1}{2}}^2}, \quad (\text{S5})$$

$$\tilde{u}_2 = \eta_{\frac{1}{2}} \sqrt{\frac{3j}{4(j+1)}} \sqrt{1 - \eta_{\frac{3}{2}}^2}, \quad (\text{S6})$$

$$\tilde{v}_1 = \frac{\sqrt{3}}{2j} \sqrt{\left(j - \frac{1}{2} \right) \left(j + \frac{3}{2} \right)} \sqrt{\left(1 - \eta_{-\frac{1}{2}}^2 \right) \left(1 - \eta_{\frac{1}{2}}^2 \right)}, \quad (\text{S7})$$

$$\tilde{v}_2 = \frac{\sqrt{3}}{2(1+j)} \sqrt{\left(j - \frac{1}{2} \right) \left(j + \frac{3}{2} \right)} \sqrt{\left(1 - \eta_{\frac{1}{2}}^2 \right) \left(1 - \eta_{\frac{3}{2}}^2 \right)}, \quad (\text{S8})$$

$$\tilde{w} = \frac{3}{2} \sqrt{\frac{1}{j(j+1)}} \sqrt{\eta_{\frac{3}{2}}\eta_{-\frac{1}{2}} \left(1 - \eta_{\frac{1}{2}}^2 \right)} \quad (\text{S9})$$

Taking the limit of $Q \rightarrow \infty$, and keeping $R\sqrt{Q} = w$, $j = Q - 3/2 + n$, after some algebraic transformations, we re-write Eq. (S1) in the following form:

$$\hat{M} \begin{pmatrix} rR_1(r) \\ irR_2(r) \\ -rR_3(r) \\ -irR_4(r) \end{pmatrix} = E \begin{pmatrix} rR_1(r) \\ irR_2(r) \\ -rR_3(r) \\ -irR_4(r) \end{pmatrix}, \quad (\text{S10})$$

with the matrix operator

$$\hat{M} = \begin{pmatrix} -\frac{1}{2m_h} \frac{\partial^2}{\partial r^2} + \gamma_+(n-1) - \frac{3\gamma}{2} & -i\gamma\sqrt{6(n-2)} \frac{\partial}{\partial r} & -\gamma\sqrt{3(n-1)(n-2)} & 0 \\ -i\gamma\sqrt{6(n-2)} \frac{\partial}{\partial r} & -\frac{1}{2m_l} \frac{\partial^2}{\partial r^2} + \gamma_-n + \frac{3\gamma}{2} & 0 & -\gamma\sqrt{3n(n-1)} \\ -\gamma\sqrt{3(n-2)(n-1)} & 0 & -\frac{1}{2m_l} \frac{\partial^2}{\partial r^2} + \gamma_-(n+1) - \frac{3\gamma}{2} & -i\gamma\sqrt{6n} \frac{\partial}{\partial r} \\ 0 & -\gamma\sqrt{3n(n-1)} & -i\gamma\sqrt{6n} \frac{\partial}{\partial r} & -\frac{1}{2m_h} \frac{\partial^2}{\partial r^2} + \gamma_+(n+2) - \frac{3\gamma}{2} \end{pmatrix}, \quad (\text{S11})$$

where $\gamma_{\pm} = \gamma_1 \pm \gamma$, $m_h = (\gamma_1 - 2\gamma)^{-1}$ and $m_l = (\gamma_1 + 2\gamma)^{-1}$. This is exactly the equation for the envelope z -functions in a planar geometry. Thus, we have shown that in the limit of very large radius and monopole limit ($R, Q \rightarrow \infty$ with $R/\sqrt{Q} = w$) the wavefunctions in a spherical shell converge to the planar limit.

Zeemann term in a spherical shell geometry

We include the pure Zeeman term $\mathcal{H}_Z = \kappa \mathbf{s} \cdot \mathbf{H} / |H|$ of the Luttinger Hamiltonian that is due to direct coupling of the spin 3/2 of holes with a magnetic field, where energy is in the units of the free electron cyclotron energy and κ is the Luttinger constant. For a spherical shell, a magnetic field is not a constant in the radial direction. However, we evaluate Zeeman term approximating its value by taking the magnetic field value on the sphere of radius R , half way between the inner and outer spherical boundaries of the shell. This choice recovers the planar Zeeman term in the large Q limit. The Zeemann term is diagonal in the angular momentum representation and its eigenvalues correspond to spin projections $\pm 1/2, \pm 3/2$ in the limit of large Q . The angular part of the wavefunction is

$$\psi_{Qjm}(\theta, \phi) = \begin{pmatrix} \langle j, m | l, m - \frac{3}{2}; \frac{3}{2}, +\frac{3}{2} \rangle Y_{Q,l,m-\frac{3}{2}}(\theta, \phi) \\ \langle j, m | l, m - \frac{1}{2}; \frac{3}{2}, +\frac{1}{2} \rangle Y_{Q,l,m-\frac{1}{2}}(\theta, \phi) \\ \langle j, m | l, m + \frac{1}{2}; \frac{3}{2}, -\frac{1}{2} \rangle Y_{Q,l,m+\frac{1}{2}}(\theta, \phi) \\ \langle j, m | l, m + \frac{3}{2}; \frac{3}{2}, -\frac{3}{2} \rangle Y_{Q,l,m+\frac{3}{2}}(\theta, \phi) \end{pmatrix}, \quad (\text{S12})$$

where $\langle j, m_j | l, m - l; \frac{3}{2}, m_s \rangle$ are the Clebsch-Gordan coefficients of $\mathbf{j} = \mathbf{l} + \mathbf{s}$. In the presence of a radial magnetic field, $\mathcal{H}_Z = \kappa s_r$, where s_r is the radial component of 3/2 spin matrix, and the non-zero matrix elements of the Zeemann interaction are

$$\begin{aligned} \langle \psi_{Q,l+3/2,m} | \kappa s_r | \psi_{Q,l+3/2,m} \rangle &= 3\kappa(j - 3/2)/2Q, \\ \langle \psi_{Q,l+1/2,m} | \kappa s_r | \psi_{Q,l+1/2,m} \rangle &= \kappa(j - 7/2)/2Q, \\ \langle \psi_{Q,l-1/2,m} | \kappa s_r | \psi_{Q,l-1/2,m} \rangle &= -\kappa(j + 9/2)/2Q, \\ \langle \psi_{Q,l-3/2,m} | \kappa s_r | \psi_{Q,l-3/2,m} \rangle &= -3\kappa(j + 5/2)/2Q. \end{aligned} \quad (\text{S13})$$

Matrix elements of hole-hole Coulomb interactions

We derive the matrix elements of the hole-hole interactions by using the angular momentum addition and the relation [S1]:

$$\frac{1}{|\mathbf{r}_1 - \mathbf{r}_2|} = 4\pi \sum_{k=0}^{\infty} \sum_{\mu=-k}^k \frac{1}{2k+1} \frac{r_{<}^k}{r_{>}^{k+1}} Y_{k\mu}^*(\theta', \phi') Y_{k\mu}(\theta, \phi), \quad (\text{S14})$$

where \mathbf{r}_2 , $r_{</>}$ being the smaller (or bigger) of r_1 and r_2 , and $Y_{k\mu}(\theta, \phi)$ is a spherical function, which is a monopole harmonics function $Y_{Q=0,k,\mu}(\theta, \phi)$. A straightforward calculation by using the integral of the three monopole harmonic functions (Eq. (1) of [S2]) leads to:

$$\begin{aligned}
\langle Q; \alpha'_1, j_1, m_1 - \eta; \alpha'_2, j'_2, m_2 + \eta \mid \frac{e^2}{\epsilon |\mathbf{r}_1 - \mathbf{r}_2|} \mid Q; \alpha_1, j_1, m_1; \alpha_2, j_2, m_2 \rangle = & \frac{e^2}{\epsilon} \sum_{\mu'_1, \mu'_2} \sum_{\mu_1, \mu_2} \sum_{\sigma_1, \sigma_2} \sum_{k=0}^{\infty} (-1)^{\eta} \times \\
& \langle j'_1 + \mu_1, m_1 - \sigma_1 - \eta; \frac{3}{2}, \sigma_1 \mid j'_1, m_1 - \eta \rangle \langle j'_2 + \mu_2, m_2 + \eta - \sigma_2; \frac{3}{2}, \sigma_2 \mid j'_2, m_2 + \eta \rangle \langle j_1 + \mu_1, m_1 - \sigma_1; \frac{3}{2}, \sigma_1 \mid j_1, m_1 \rangle \\
& \langle j_2 + \mu_2, m_2 - \sigma_2; \frac{3}{2}, \sigma_2 \mid j'_2, m_2 \rangle \langle k, 0; j_1 + \mu_1, Q \mid j'_1 + \mu'_1, Q \rangle \langle j'_1 + \mu'_1, \sigma_1 + \eta - m_1; k, -\eta \mid j_1 + \mu_1; -m_1 + \sigma_1 \rangle \\
& \langle k, 0; j_2 + \mu_2, Q \mid j'_2 + \mu'_2, Q \rangle \langle j'_2 + \mu'_2, \sigma_2 + \eta - m_2; k, -\eta \mid j_2 + \mu_2; -m_2 + \sigma_2 \rangle \int_{\sqrt{Q-w}}^{\sqrt{Q+w}} \int_{\sqrt{Q-w}}^{\sqrt{Q+w}} dr_1 dr_2 r_1^2 r_2^2 \frac{r_1^k}{r_2^{k+1}} \\
& R_{j'_1}^{j'_1 + \mu'_1}(r_1) R_{j_1}^{j_1 + \mu_1}(r_1) R_{j'_2}^{j'_2 + \mu'_2}(r_2) R_{j_2}^{j_2 + \mu_2}(r_2). \tag{S15}
\end{aligned}$$

Evaluating this equation, we use explicitly known expressions for the Clebsch-Gordan coefficients, and numerically calculate the integrals by applying Simpson rule for evaluating the numerical quadrature involving radial wavefunctions.

Two- and three-body pseudopotentials of the hole-hole interaction

TABLE I: Corrections due to LL mixing to the ground state two-body pseudopotentials in units of $e^4/\epsilon^2 \ell^2 \hbar \omega_C^0$

$L/2\ell$	1.4	1.5	1.6	1.7	1.8	1.9	2.0
$\delta V_5 - \delta V_3$	0.0248	0.0211	0.0187	0.0168	0.0153	0.0140	0.0129
$\delta V_7 - \delta V_3$	0.0314	0.0266	0.0235	0.0212	0.0192	0.0176	0.0161

TABLE II: The ground state irreducible three-body pseudopotentials in units of $e^4/\epsilon^2 \ell^2 \hbar \omega_C^0$

$L/2\ell$	1.4	1.5	1.6	1.7	1.8	1.9	2.0
$\tilde{V}_5 - \tilde{V}_3$	0.0015	0.0108	0.0150	0.0174	0.0188	0.0196	0.0202
$\tilde{V}_6 - \tilde{V}_3$	-0.0357	-0.0240	-0.0177	-0.0136	-0.0107	-0.0086	-0.0070

* Electronic address: simion@purdue.edu

† Electronic address: yuli@purdue.edu

[S1] J. D. Jackson, *Classical electrodynamics* (Wiley, New York, NY, 1999), 3rd ed., ISBN 9780471309321.

[S2] T. T. Wu and C. N. Yang, Phys. Rev. D **16**, 1018 (1977).